Submitted to the 1st IEEE/RAS-EMBS Int. Conf. on
Biomedical Robotics and Biomechatronics (BioRob 2006), Pisa, Italy, February 20-22, 2006

Biomimetic Centering for Undulatory Robots*

Michael Sfakiotakis, Dimitris P. Tsakiris and Anastasios Vlaikidis
Computational Vision and Robotics Laboratory
Institute of Computer Science - FORTH
Vassilika Vouton, P.O. Box 1385, GR-71110 Heraklion, Greece
{*sfakios, tsakiris, agblaiki*}*@ics.forth.gr*

***Abstract*— Substantial work exists in the undulatory robotics literature on the mechanical design, modeling, gait generation and implementation of robotic prototypes. However, there appears to have been relatively limited work on the use of exteroceptive sensors in control schemes leading to more complex reactive undulatory behaviors. This paper considers a biologically-inspired sensor-based centering behavior for undulatory robots, originally developed for nonholonomic mobile robots. Adaptation to the significantly more complex dynamics of undulatory locomotors highlights a number of issues related to the use of sensors, possibly distributed over the elongated body of the mechanism, for the generation of reactive behaviors, to biomimetic neuromuscular control and to formation control of multi-undulatory swarms. These issues are explored via computational tools specifically geared towards undulatory locomotion in robotics and biology.**

***Index Terms*— biomimetic robotics, undulatory locomotion, reactive behaviors, exteroceptive sensors.**

I. Introduction

Undulatory robotic locomotors are serially connected, multilink articulated mechanisms, which propel themselves by body shape undulations. Advantages associated with them include terrain adaptability, modularity and redundancy, as well as their potential for use as combined locomotors and manipulators. Inspiration for the design and development of such mechanisms is provided by biological organisms, as locomotion by transversal whole-body waves is widespread among elongated, narrow animals (snakes, eels, marine worms, larvae, etc.). While most of the existing such robots utilize passive wheels to realize serpentine locomotion (see [1]–[5] and references therein), more recent work addresses undulatory prototypes which crawl on their underside, and do not rely on wheels (e.g., [6]–[10]), as well as undulatory swimming robots (e.g., [2], [11]–[13]).

The literature on undulatory robotics has mainly focused on mechanical design and open-loop control. However, in order for such devices to be able to operate in the complex environments for which they are intended, they should be equipped with exteroceptive sensors allowing the implementation of more complex behaviors, either for single robots (e.g., obstacle avoidance, pursuit of moving targets), or for multi-robot swarms (e.g., formation control, cooperative exploration). The ACM-III wheeled serpentine robot, equipped with many tactile sensors along its body, demonstrated advancement along narrow labyrinths and adaptive coiling around objects [1]. The GMD snake-like robots featured tactile sensors, infrared sensors for use in path planning, cameras and lasers adapted to pipeline inspection, etc. [6], [14], [15]. The lamprey robot of [11] used both proprioceptive (compass, inclinometers) and exteroceptive sensors (sonars), to allow behavior switches in response to environment perturbations. Simulations of gaits for traversing complex environments, involving the use of distance sensors distributed along the body of an undulatory mechanism, are presented in [16].

Many potential applications for undulatory robots (e.g., site inspection, search-and-rescue missions, mine clearance) involve tasks which could be efficiently addressed by multiple robotic agents operating as a swarm. A significant body of work is available regarding the dynamics and control of such swarms for conventional mobile robots, underwater vehicles and aerial vehicles [17]–[22]. Sensor-based aspects of these control problems are addressed in e.g., [19]–[21]. However, swarms of undulatory robots do not appear to have been investigated.

This paper considers a biologically-inspired sensor-based centering behavior for undulatory robots. This reactive robotic behavior, observed and studied in bees, was originally developed for nonholonomic mobile robots [23]. Adaptation to the significantly more complex dynamics of undulatory locomotors is discussed in Section III, and highlights various issues related to the use of sensors, possibly distributed over the elongated body of the mechanism, for the generation of reactive behaviors. These issues are explored via the SIMUUN set of computational tools, which are specifically geared towards undulatory locomotion in robotics and biology [24]. Simulation results related to undulatory centering, implemented both via explicit shape angle control and via biomimetic neuromuscular control, and to formation control of multi-undulatory swarms are presented in Section IV.

II. Modelling Undulatory Locomotion

Undulatory locomotion is achieved through appropriate coupling of internal shape changes (typically a wave traveling along the body) to external motion constrains (typically frictional forces arising from the interaction with the locomotion environment). The main components

*This work was supported in part by the European Commission, through the Future and Emerging Technologies program (IST-FET), under grant IST-2001-34181 (project BIOLOCH).

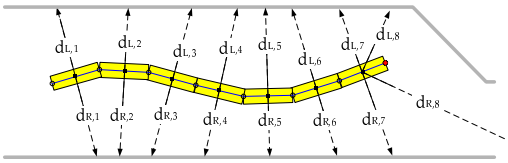

Fig. 1. Computational model of a seven-link undulatory mechanism and its sensor array.

involved in simulating an undulatory locomotor are: (i) the body mechanical model, (ii) the force model of the body's interaction with the environment and (iii) the body shape control strategy. In the present study, undulatory locomotors are modeled as articulated robots comprising serially connected, rigid 2D links, interconnected by planar revolute joints. Details of the system's Euler-Lagrange equations of motion appear in [10]. A viscous friction model is used for the interaction of individual links with the environment, in which the two components of the force applied to the ith link are respectively obtained as:

$$F_T^i = -c_T \cdot v_T^i \quad \text{and} \quad F_N^i = -c_N \cdot v_N^i, \tag{1}$$

where v_T^i and v_N^i are the tangential and normal components of the velocity of the ith link. The ratio c_N/c_T of the force coefficients is a key parameter in undulatory locomotion. For $c_N > c_T$ the overall locomotion direction is *opposite* to that of the wave direction; therefore, forward propulsion is achieved by a head-to-tail body wave. This type of *eel-like* undulatory locomotion is by far the most common in nature, both on land and in the sea, and has been replicated in the vast majority of existing serpentine robots. For $c_N < c_T$ the locomotion is *along* the direction of wave propagation; hence forward motion is achieved by a tail-to-head wave. In nature, this locomotion mode is exhibited by the polychaete annelid marine worms. A robotic prototype implementing this novel type of *polychaete-like* undulatory locomotion is described in [10].

The body shape control component is responsible for generating a traveling wave along the mechanism. The two methods employed for this purpose in the present study are:

1) Explicit joint angle control: The most straightforward way to explicitly generate a traveling wave in a serial chain of N links is by having the $N-1$ joint angles vary sinusoidally, with a common frequency f and a constant phase lag ϕ_{lag} between consecutive joints:

$$\phi_i(t) = A\sin(2\pi f t + i\phi_{lag}) - \psi_i, \tag{2}$$

where A is the joint oscillation amplitude. Note that this approach implies full control of the mechanism's joint angles, without consideration of the required torques. The angular offset ψ_i provides a means for steering along curved paths, and is set to $\psi = 0$ for locomotion along a straight line. The propagation direction for the wave depends on the sign of the phase lag parameter, and is from link-N to link-1 for $\phi_{lag} > 0$. The condition $\phi_{lag} = \pm 2\pi/N$ yields (exactly) one wavelength of the propulsive wave across the undulating body, with beneficial effects on the propulsive efficiency. For links of identical length l, the formulation of (2) produces a sinusoid-like body shape (shown in Fig. 3 for a seven-link mechanism) which is an approximation of the *serpenoid curve* introduced in [1]; the equations provided therein can be used to obtain estimates of the body wave amplitude B as a function of A and N, when $\phi_{lag} = 2\pi/N$:

$$B = L\int_0^{1/4} \sin\left(\frac{A}{2\,|\sin(\pi/N)|}\cos(2\pi\sigma)\right) d\sigma, \tag{3}$$

where $L = Nl$ is the total length of the mechanism. This is shown in Fig. 2.

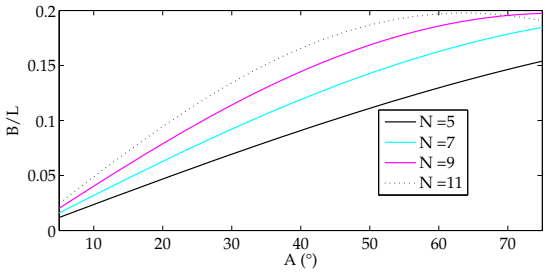

Fig. 2. The body wave amplitude B (normalized by the body length L), as a function of the joint angle amplitude A and the number of links N.

Closed-loop control schemes utilizing (2) may be set up, where the parameters A and/or f are used to modify the speed of locomotion, while changes in ψ alter the orientation.

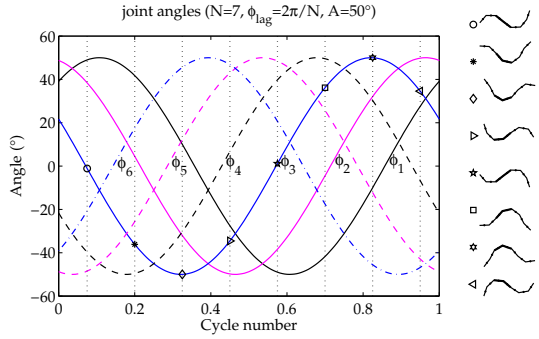

Fig. 3. Relation between the joint angles and the overall body shape for the explicit joint angle control scheme.

2) Neural control: Neuromuscular body shape control schemes have been developed, based on models of the central pattern generator (CPG) which controls the undulatory swimming of the lamprey (e.g., [25], [26]). These implement a connectionist CPG circuit, which is modelled as a chain of (identical) segmental oscillators, properly interconnected to generate a wave of joint activation. Each segmental oscillator comprises interneurons and motoneurons (all of which are modelled as leaky integrators), arranged in two symmetrical sub-networks that create oscillations

through mutual inhibition. The torque eventually applied to each of the body joints is determined by the outputs of the corresponding motoneurons, after they activate a pair of antagonistic lateral muscles, which are simulated using a spring-and-damper muscle model. The characteristics of the motoneuron outputs can be altered by tonic (i.e., non-oscillating) inputs to the left and right sub-networks of the segmental oscillators (I_L and I_R, respectively) [9]. When this neuromuscular control scheme is coupled to the body's mechanical model, motion in a straight line is obtained by symmetric activation of the two sides of the body CPG (i.e. for $I_L = I_R$), while turning motions are instigated by unequal tonic input to them. Since the CPG-based approach provides torque signals to the joints, their exact angular motion depends on the mechanical properties of the segments, as well as on the parameters of the force model used.

Despite the considerably increased computational complexity of the CPG-based neural control scheme, a number of appealing characteristics (distributed architecture, potential robustness through redundancy, etc.) render it an interesting alternative for motion control of undulatory robots.

III. Reactive Behaviors for Undulatory Robots

The elongated articulated body of undulatory robots, whose locomotion involves a continuously changing shape, complicates the generation of reactive behaviors. Systematic guidelines for the selection of parameters like the number, type and topology of sensors are currently lacking; however, the typically modular nature of these robots hints at a distributed sensing and control system. The approach adopted here considers proximity sensors placed on each link of the robot, which are employed to dynamically adjust the propulsive wave amplitude. The head link incorporates additional sensors (e.g., vision), whose output is utilized in steering the mechanism. This approach parallels the distribution of sensory structures in e.g., polychaete annelid worms [27].

Simulations presented in this study consider an undulatory mechanism comprising $N = 7$ identical links, each equipped with a distance sensor pair aiming at $\pm 90^\circ$ with respect to the link's main axis, while the head link features an additional distance sensor pair, aiming at $\pm 45^\circ$ (Fig. 1).

A. Reactive Centering Control

The reactive behavior presented here is inspired by the centering response exhibited by bees when flying through narrow gaps, which has been attributed to their balancing the retinal motion perceived by each of their two wide field-of-view compound eyes. This has inspired the implementation of reactive centering schemes for nonholonomic mobile robots, where optical flow information from several distinct "looking" directions in the field of view of an onboard panoramic camera is employed directly in the control loop [23]. The mobile robot is assumed to be moving inside a "corridor" formed by obstacles, which can be locally approximated by two straight parallel walls. The task of implementing a centering response consists in using the angular velocity ω of the mobile robot to drive the lateral distance of the robot from the walls, as well as its orientation, to desired values corresponding to the middle of the corridor. Inspired by the bee centering response, a motion control scheme, asymptotically driving the scaled difference of inverse depths of the robot from the corridor walls to zero, can be shown to effectively address this problem. Adaptation of this sensor-based control scheme to the dynamics of undulatory robotic locomotors relies on balancing the weighted sum of the distance sensor outputs to the left and right sides of the robot. Assuming M pairs of distance sensors, and denoting by $d_{L,j}$ and $d_{R,j}$ ($1 \leq j \leq M$) the outputs for such a sensing array (Fig. 1), a steering offset is obtained using the distance metric $s(t)$, which is calculated as:

$$s(t) = \frac{1}{\sum_{j=1}^{M} w_j d_{L,j}(t)} - \frac{1}{\sum_{j=1}^{M} w_j d_{R,j}(t)}. \quad (4)$$

The weights w_j in (4) determine the relative contribution of each of the M sensor pairs in calculating $s(t)$. For the explicit joint angle control scheme, the steering offset for the ith joint angle is then obtained as $\psi_i(t) = g s(t)$. Therefore, the full joint angle control comprises a periodic component (first term below) and a sensor-based feedback component (second term), i.e.:

$$\phi_i(t) = A \sin(2\pi f t + i\phi_{lag}) - g s(t). \quad (5)$$

For the neural control scheme, $s(t)$ is used to alter the tonic input signals applied to the left and right sides of the CPG, so that:

$$I_L(t) = 1 - k s(t) \quad \text{and} \quad I_R(t) = 1 + k s(t), \quad \text{for } k > 0. \quad (6)$$

B. Reactive Modulation of Undulatory Envelope

Reactive envelope modulation refers to the use of information from sensors distributed along the undulatory mechanism to adjust the amplitude of the body wave, in order to allow the robot to navigate in environments involving tighter turns and/or variable corridor widths. Assuming ideal distance sensors, the approach adopted involves an adaptive gain $p(t)$ multiplying all joint angle controls $\phi_i(t)$, which depends on the instantaneous value of the proximity ratio $B/d_{\min}$ ($d_{\min}$ is the minimum value of the distance sensors' output and B is the body wave amplitude):

$$p(t) = k_1 + \frac{1}{T} \int_{t-T}^{t} \frac{k_2 - k_1}{1 + \exp\left(-c_1 \dfrac{B(t)}{d_{\min}(t)} + c_2\right)} dt. \quad (7)$$

This implements an asymmetric sigmoid gain of the proximity ratio (k_2 and k_1 are the upper and lower asymptotic values, while the slope and the point of unit gain is specified via c_1 and c_2; see Fig. 4), subsequently smoothed by a moving average filter which spans the joint oscillation

period $T = 1/f$. The filtering stage improves robustness over abrupt changes in $d_{\min}$ (brought about e.g., by tight turns in complex structures) at the expense of reduced responsiveness.

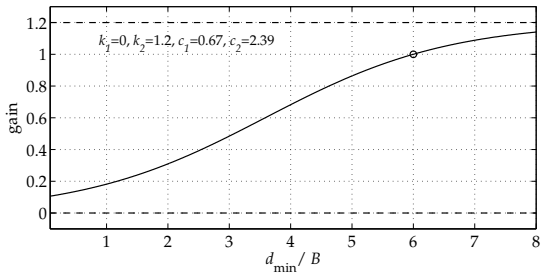

Fig. 4. The asymmetric gain as a function of the proximity ratio.

For the neural control scheme, modulation of the undulatory envelope can be obtained by applying a similar adaptive gain to both tonic input signals controlling the body CPG. Note however, that the required mapping of the tonic excitation level to the resulting body wave amplitude of the undulatory mechanism cannot be performed analytically and needs to be experimentally determined.

Variations of these approaches can be used for centering and for modulating the undulatory envelope, also when the proximity information is provided by simpler sensing elements (e.g., whisker-like tactile switches).

IV. Simulation Results

Simulations implementing the reactive behaviors proposed above are set up using the SIMUUN simulation environment, which provides tools for deploying computational models of undulatory locomotion within a Matlab/Simulink framework [24]. SIMUUN also includes modules which emulate distance sensing elements, as well as implement simple 2D models of the world that the mechanism operates in. These are used to set up the sensor array for the seven-link mechanism (Fig. 1), and to construct corridor-like environments of varying complexity to test the performance of the centering controller, both for the explicit joint angle control and for the CPG-based methods of generating the traveling wave.

A. Undulatory Centering with Explicit Joint Angle Control

The efficacy of the undulatory centering controller utilizing (4)-(5) was investigated in a series of simulations, carried out over a range of c_N/c_T values that involved both eel-like and polychaete-like interaction with the environment. The body wave parameters were set as $A = 28°$, $phi_{lag} = 2\pi/N$, and simulations were performed for different values of the controller gain in (5), initially considering the geometry of parallel-sided corridors with a width equal to L or $2L$.

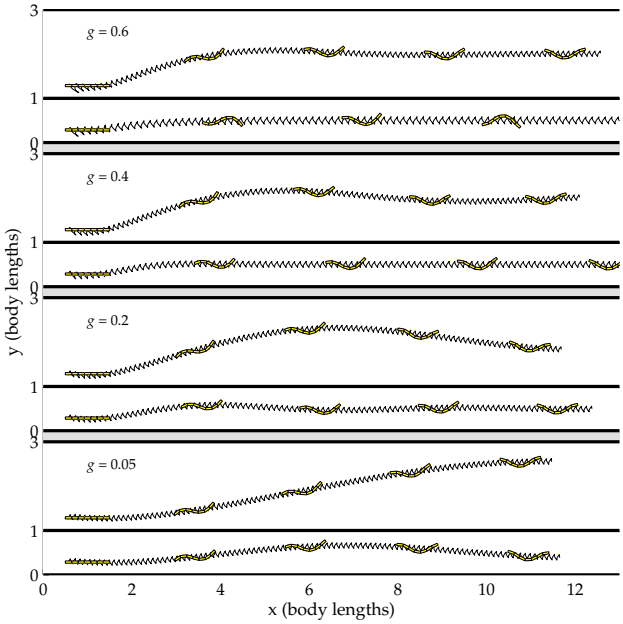

Fig. 5. Centering behavior utilising sensor data from only the head link, for polychaete-like interaction with the environment ($c_N/c_T = 0.025$).

Utilizing data only from the head sensors, the centering behavior was found to be successfully implemented for both eel-like and polychaete-like undulatory locomotion. The speed of convergence along the center of the corridor was found to depend both on the gain g and on the corridor width, while the c_N/c_T ratio had little impact on the trajectory followed. Fig. 5 illustrates these points for polychaete-like locomotion, while the ability of the same control scheme to generate the centering behavior on areas comprising different types of interaction is demonstrated in Fig. 6.

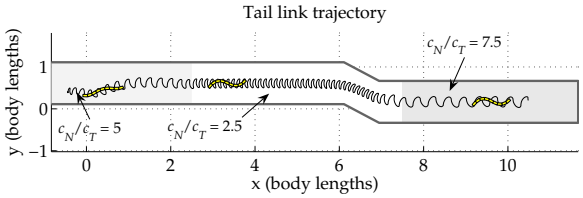

Fig. 6. Undulatory centering behavior over a locomotion environment with differing frictional characteristics (shown for eel-like interaction with the environment).

Envelope Modulation

Incorporating the sensor-based envelope modulation scheme allows navigation of the complex corridor-like structure in Fig. 7, without the mechanism coming into contact with the corridor walls; this is not the case when using the steering controller alone. An additional consequence is the ability to increase the undulation amplitude (and therefore the locomotion speed) when traversing wider corridor sections.

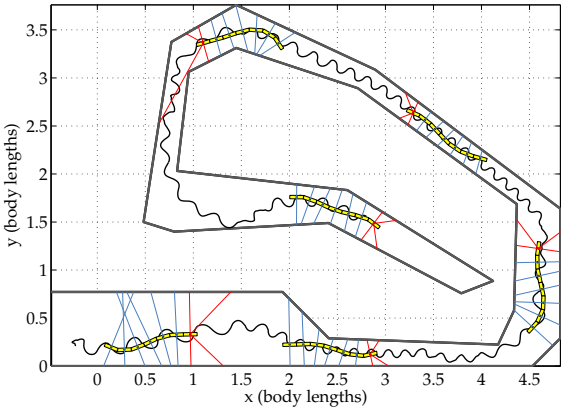

(a) - tail link trajectory

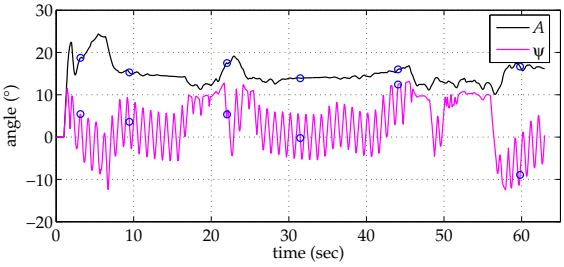

(b) - body wave controls

Fig. 7. Combining reactive centering and envelope modulation to navigate a complex corridor. The nominal joint oscillation amplitude (i.e. corresponding to $p(t) = 1$) is $A_0 = 30°$. In the trajectory plot, blue lines denote the sensed distances which are used for envelope modulation alone.

B. Undulatory Centering with Neural Control

The reactive centering behavior may be implemented in a more biomimetic way using neuromuscular control schemes via an appropriate CPG neural circuit. This comprises 20 segmental oscillators, with the motoneuron outputs from (roughly) every third oscillator utilized to provide torque signals to the six joints of the seven-link mechanism, through the spring-and-damper model of antagonistic muscle activation. A series of simulations demonstrates the ability of the integrated neural control scheme to successfully navigate the robot through various corridor-like courses, both for eel-like and for polychaete-like interaction with the environment, when utilizing sensory information from the head link. Indicative results are shown in Figs. 8-9.

C. Formation Control of Undulatory Swarms

Simulations of multiple undulatory mechanisms, each implementing the reactive centering behavior, were also carried out, demonstrating that the scheme is well suited to the task of having such a swarm traverse corridor-like environments. In particular, when the swarm configuration involved two or more mechanisms moving alongside, a distribution of them along the corridor width emerged as a consequence of each one essentially forming a moving boundary for the centering behavior of the adjacent mechanisms. Integrating reactive envelope modulation with the centering control in each undulatory mechanism affords improved collision avoidance and greater versatility with

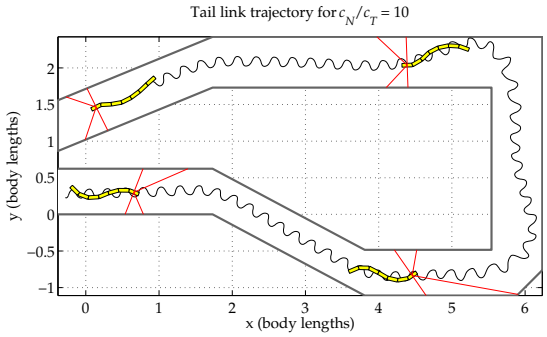

Fig. 8. Neural control of the undulatory centering behavior, for eel-like locomotion. The gain in (6) is $k = 0.029$.

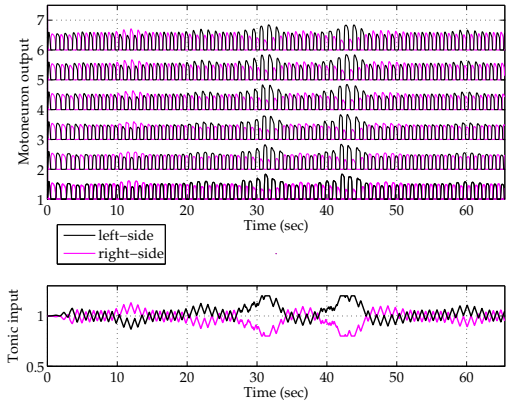

Fig. 9. Neural control of the undulatory centering behavior for eel-like locomotion: Tonic inputs (bottom) and the respective motoneuron outputs (top) for the simulation run shown in Fig. 8.

regard to the complexity of the course to be traversed. Increased swarm coherence may be obtained by implementing appropriate formation control laws, in addition to the centering behavior. Here we employ a variation of the "rectilinear" controller proposed in [19], [20] for multiple unit-speed vehicles, where formations emerge by steering controls alone. Adaptation to a swarm of undulatory mechanisms, each under explicit joint angle control, involves setting the steering offset in (2) for the jth robot according to the following expression:

$$\psi_j = \frac{1}{n}\sum_{k\neq j}(-\eta \sin\varphi_j \cos\varphi_j + f(\rho_{jk})\cos\varphi_j + \mu \sin(\varphi_k - \varphi_j)), \tag{8}$$

where n is the number of mechanisms. Considering a pair of undulatory robots, ρ_{jk} denotes the distance between their head link centers, while φ_j and φ_k is the orientation of the head links with respect to the direction perpendicular to the baseline connecting the centers of the head links. In undulatory robotic prototypes, such sensory information might be obtained e.g., by a combination of panoramic cameras (for determining the relative orientation) and scanning laser sensors (for obtaining range estimates). Indicative results from the SIMUUN simulations, involving undula-

tory robots under both formation and centering control, are shown in Fig. 10.

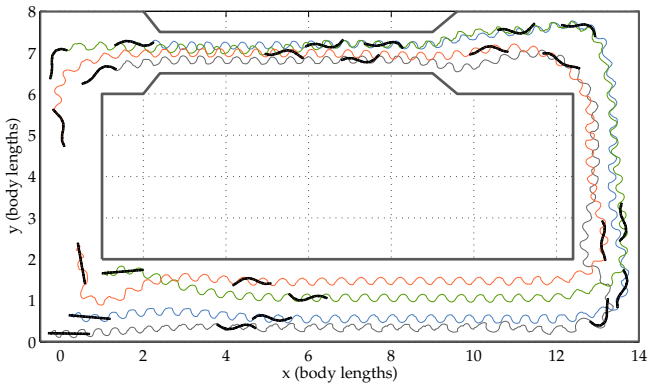

Fig. 10. Swarm of undulatory robots maintains its cohesion in a corridor environment.

V. Conclusions and Future Work

Several control schemes, giving rise to closed-loop reactive behaviors for undulatory robots, have been presented and evaluated in simulation. A biomimetic centering behavior has been implemented, both by explicit body shape control, as well as by neuromuscular control of body undulations. Formation control for swarms of multiple undulatory robots has been demonstrated in narrow corridor-like environments; in conjunction with centering control, the swarm robots are able to maintain the cohesion of their group while navigating successfully in these environments. In related work, an eleven-link polychaete-like robotic prototype has been developed for the investigation of undulatory locomotion; experiments performed with it show good agreement with the SIMUUN computational models [10]. This provides early evidence regarding the plausibility of the presented reactive control schemes for undulatory robots, which are expected to be tested experimentally in the future with appropriate prototypes equipped with distance and vision sensors.

References

[1] S. Hirose, *Biologically Inspired Robots: Snake-Like Locomotors and Manipulators*. New York: Oxford University Press, 1993.

[2] S. Hirose and E. Fukushima, "Snakes and strings: New robotic components for rescue operations," *Int. J. Robot. Res.*, vol. 23, no. 4/5, pp. 341–349, 2004.

[3] J. Ostrowski and J. Burdick, "The geometric mechanics of undulatory robotic locomotion," *Int. J. Robot. Res.*, vol. 17, no. 7, pp. 683–701, 1998.

[4] S. Ma, "Development of a creeping locomotion snake-robot," *Int. J. Robot. Automat.*, vol. 17, no. 4, pp. 146–153, 2002.

[5] P. Krishnaprasad and D. Tsakiris, "Oscillations, SE(2)-snakes and motion control: A study of the roller racer," *Dyn. Syst.*, vol. 16, no. 4, pp. 347–397, 2001.

[6] R. Worst and R. Linnemann, "Construction and operation of a snake-like robot," in *Proc. IEEE Int. Joint Symp. on Intelligence and Systems*, 1996, pp. 164–169.

[7] M. Saito, M. Fukaya, and T. Iwasaki, "Modeling, analysis, and synthesis of serpentine locomotion with a multilink robotic snake," *IEEE Control Syst. Mag.*, vol. 22, no. 1, pp. 64–81, 2002.

[8] L. Chen, S. Wang, S. Ma, and B. Li, "Analysis of traveling wave locomotion of snake robot," in *Proc. IEEE Int. Conf. on Robotics, Intelligent Systems and Signal Processing (RISSP'03)*, Changsha, China, 2003, pp. 365–369.

[9] D. Tsakiris, A. Menciassi, M. Sfakiotakis, G. La Spina, and P. Dario, "Undulatory locomotion of polychaete annelids: mechanics, neural control and robotic prototypes," presented at The Annual Computational Neuroscience Meeting, Baltimore, USA, 2004.

[10] D. Tsakiris, M. Sfakiotakis, A. Menciassi, G. La Spina, and P. Dario, "Polychaete-like undulatory robotic locomotion," in *Proc. IEEE Int. Conf. on Robotics and Automation (ICRA'05)*, Barcelona, Spain, 2005, pp. 3029–3034.

[11] J. Ayers, C. Wilbur, and C. Olcott, "Lamprey robots," in *Proc. Int. Symp. on Aqua Biomechanisms*, T. Wu and N. Kato, Eds., 2000.

[12] K. McIsaac and J. Ostrowski, "Motion planning for anguilliform locomotion," *IEEE J. Robot. Automat.*, vol. 19, no. 4, pp. 637–652, 2003.

[13] A. Crespi, A. Badertscher, A. Guignard, and A. Ijspeert, "Amphibot I : an amphibious snake-like robot," *Robot. Auton. Syst.*, vol. 50, no. 4, pp. 163–175, 2005.

[14] B. Klaassen and K. Paap, "GMD-SNAKE2: A snake-like robot driven by wheels and a method for motion control," in *Proc. IEEE Int. Conf. on Robotics and Automation (ICRA'96)*, 1999, pp. 3014–3019.

[15] M. Kolesnik and H. Streich, "Visual orientation and motion control of MAKRO - adaptation to the sewer environment," in *Proc. 7th Int. Conf. on Simulation of Adaptive Behavior*, 2002, pp. 62–69.

[16] G. Kulali, M. Gevher, A. Erkmen, and I. Erkmen, "Intelligent gait synthesizer for serpentine robots," in *Proc. IEEE Int. Conf. on Robotics and Automation (ICRA'02)*, Washington, DC, USA, 2002, pp. 1513–1518.

[17] A. Jadbabaie, J. Lin, and A. Morse, "Coordination of groups of mobile autonomous agents using nearest neighbor rules," *IEEE Trans. Automat. Contr.*, vol. 48, no. 6, pp. 988–1001, 2003.

[18] P. Ögren and N. Leonard, "Obstacle avoidance in formation," in *Proc. IEEE Int. Conf. on Robotics and Automation (ICRA'03)*, Taipei, Taiwan, 2003, pp. 2492–2497.

[19] E. Justh and P. Krishnaprasad, "A simple control law for UAV formation flying," Technical Report TR-2002-38, Institute for Systems Research, University of Maryland, College Park, 2002.

[20] ——, "Equilibria and steering laws for planar formation," *Syst. Cont. Lett.*, vol. 52, no. 1, pp. 25–38, 2004.

[21] R. Vidal, O. Shakernia, and S. Sastry, "Following the flock," *IEEE Robot. Automat. Mag.*, vol. 11, no. 4, pp. 14–20, 2004.

[22] M. Dorigo et al, "Evolving self-organizing behaviors for a Swarm-bot," *Aut. Robots*, vol. 17, no. 2/3, pp. 223–245, 2004.

[23] A. Argyros, D. Tsakiris, and C. Groyer, "Biomimetic centering behavior for mobile robots with panoramic sensors," *IEEE Robot. Automat. Mag.*, vol. 11, no. 4, pp. 347–397, 2004.

[24] M. Sfakiotakis and D. Tsakiris, "SIMUUN: A simulation environment for undulatory locomotion," *Int. J. Modelling and Simulation*, IASTED/Acta Press, in press.

[25] Ö. Ekeberg and S. Grillner, "Simulations of neuromuscular control in lamprey swimming," *Philos. Trans. R. Soc. Lond. Ser. B*, vol. 354, no. 1385, pp. 895–902, 1999.

[26] A. Ijspeert, "A connectionist central pattern generator for the aquatic and terrestrial gaits of a simulated salamander," *Biol. Cybern.*, vol. 85, no. 5, pp. 331–348, 2001.

[27] R. Brusca and G. Brusca, *Invertebrates*. Sunderland: Sinauer Associates, 1990.